High Frequency Harmonic Current Generator for More Electric Aircraft Based on GaN HFETs

line 1: 1st Meiqi Wang
line 2: *Facuty of science and engineering*
line 3: *University of Nottingham Ningbo China*
line 4: Ningbo, China

line 1: 2nd Boran Fan
line 2: *Department of electrical engineering*
line 3: *Tsinghua University*
line 4: Beijing, China

line 1: 3rd Lie Xu
line 2: *Department of electrical engineering*
line 3: *Tsinghua University*
line 4: Beijing, China

line 1: 4th Kuiwang
line 2: *Department of electrical engineering*
line 3: *Tsinghua University*
line 4: Beijing, China

line 1: 5st Zedong Zheng
line 2: *Department of electrical engineering*
line 3: *Tsinghua University*
line 4: Beijing, China

line 1: 6nd Yongdong Li
line 2: *Department of electrical engineering*
line 3: *Tsinghua University*
line 4: Beijing, China

line 1: 7rd Chris Gerada
line 2: *Facuty of science and engineering*
line 3: *University of Nottingham Ningbo China; University of Nottingham.*
line 4: Ningbo China; Nottingham NG7 2RD, U.K

line 1: 8th He Zhang
line 2: *Facuty of science and engineering*
line 3: *University of Nottingham Ningbo China*
line 4: Ningbo, China

line 1: 9th Jing Li
line 2: *Facuty of science and engineering*
line 3: *University of Nottingham Ningbo China*
line 4: Ningbo, China

***Abstract*—With the development of more electric aircraft (MEA), the number of power electronic equipment and variable frequency electrical loads are increasing rapidly, which leads to challenges in terms of power quality of aircraft power system. In this paper, a harmonic current generator (HCG) for MEA power system is designed, which can realize high frequency harmonic current injection (up to 40 times of fundamental frequency, 32kHz for 800Hz power system). For the equivalent switching frequency is close to 1MHz, a GaN HFETs based cascaded H-bridge topology is selected and a frequency adaptive multi-harmonic proportional resonance controller is introduced to achieve accurate injection of harmonic currents. To verify the analysis and injection performance of the proposed HCG, the simulation model based on PLECS is developed and tested under various operating conditions. To verify the performance of the proposed HCG, a 10kW experimental prototype is built and tested in the laboratory.**

Keywords—MEA, harmonic current generator (HCG), Gallium Nitride (GaN) HFET, cascaded H-bridge converter

I. INTRODUCTION

The architecture of the conventional civil aircraft, which is composed of a combination of hydraulic, pneumatic, mechanical and electrical power systems, has some drawbacks such as low safety margin and difficulty of maintenance; the complicated and heavy mechanical and hydraulic systems could decrease the accuracy of control system and increase the consumption of aviation fuel[1][2][3]. Meanwhile, more and more commercial demands such as Seat Power Supply (SPS) and In-Flight Entertainment (IFE) lead to an increasing demand of electrical power in the current aircraft development. Under these circumstances, the concept of More Electric Aircraft (MEA) and All Electric Aircraft (AEA) have been proposed and being expected to provide significant benefits in terms of system dependability, actuation accuracy, energy efficiency, employ flexibility and overall lifecycle cost. With the increase of electrical loads and power electronic equipment and the more complex topology of the electrical power network, power quality issues draw more and more attention, which leads to a growing demand of a highly reliable, fault-tolerant, autonomously controlled electrical power system (EPS)[4].

In Fig. 1, the scheme of an aircraft electrical power system is illustrated. It can be seen, the EPS is mainly composed of two different voltage level AC buses (230V/115V) and two different voltage level DC buses (270V/28V), and the fundamental frequency is at the range of 360-800Hz (much higher than 50/60Hz standard industrial applications), which leads to a high level of harmonic frequencies (in a 400Hz constant frequency aircraft EPS, the frequencies of the 11th and 13th harmonics can be calculated as high as 4.4 and 5.2kHz, when the fundamental frequency reaches 800Hz, the level of harmonic frequencies can up to tens of kHz).

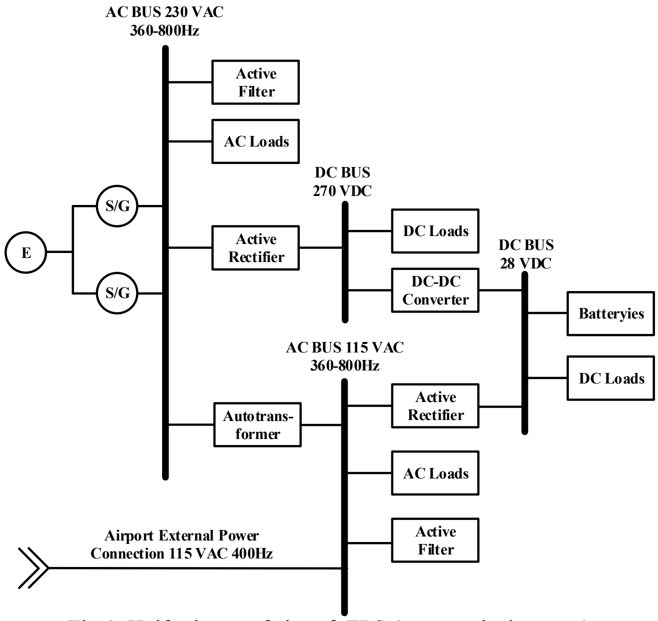

Fig 1. Half scheme of aircraft EPS (symmetrical system)

The increasing unbalance loads and power electronic devices lead to a growing quantity of high frequency harmonics. The present of harmonic distortion can cause drawbacks such as transmission power losses, conductor overheating, over loading of capacitor bank, lower power factor, etc.[5], which will affect the quality of power distribution system as well as the performance of starter/generator of MEA. Over the two decades, there were many efforts that have been made in eliminating the harmonic distortion in power system distribution such as passive power filter (PPF) [6][7] and active power filters (APFs) [8][9][10], but the high frequency of MEA power system make it different from ground power systems.

In order to figure out the influence of high frequency harmonic on aircraft power system, a harmonic current generator (HCG) is necessary for researchers to realize command harmonic current injection. In this paper, a high-performance harmonic current generator for MEA power system is proposed. The Gallium Nitride (GaN) HFETs based H-bridge is used to achieve accurate high-frequency harmonic injection. In order to achieve a wide range of injection current frequency, a control strategy based on α-β stationary reference frame (SRF) and proportional resonating (PR) controller is proposed. To verify the analysis and injection performance of the proposed HCG, the simulation model based on PLECS is developed and tested under various operating conditions. For further study, a 10kw experimental prototype is built and tested in the laboratory.

II. Control Strategy of the Proposed HCG

The harmonic current generator designed in this paper is looking forward to realize both symmetry and asymmetry injection of the harmonic current with adjustable amplitude and phase. To realize multi harmonic injection at the same time, the conventional synchronous frame PI controller can hardly be used on fixed-point processor due to the multiple frame transformations.

A. *Frequency adaptive multi-harmonic PR controller*

In order to overcome the computational burden and realize the accurate injection of various harmonic currents, a control method based on the stationary α-β frame and proportional resonant (PR) controller is introduced. Many researchers have introduced PR controller to power electronics converters in the past years, analysis its advantages and disadvantages [11][12]. As a stationary frame AC regulator, PR controller can achieve zero steady-state error and be directly applied to AC signals provides an effective solution to this application. Although applied in different coordinate systems, the nature of PR controller and PI controller is inevitably linked, and according to the transfer function of synchronous frame, the open-loop transfer function of stationary frame can be obtained.

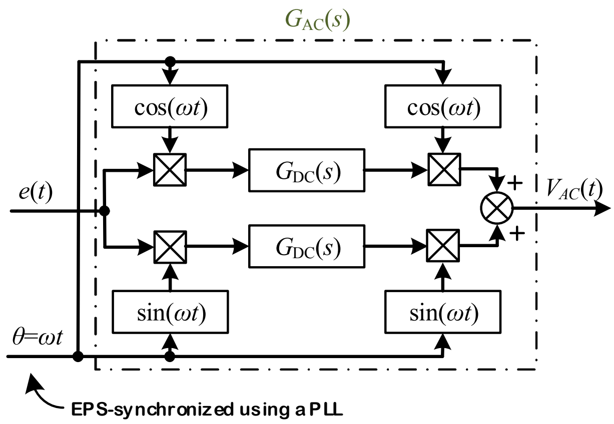

Fig. 2 Single-phase equivalent representation of synchronous frame PI and stationary frame PR controllers

Take for example, in figure 2, a single-phase equivalent representation of synchronous frame PI and stationary frame PR controllers is illustrated. It can be seen, for single-phase PI control, the synchronous d-q transformation cannot be applied directly, by increasing a demodulator and modulator (multiplying the e(t) by sine and cosine functions, as shown in figure 3) to the control system, the PI control can be applied with the transfer function $G_{DC}(s)$ [13]. The system can be described in the time-domain as follow [14][15]:

$$v_{AC}(t) = \left\{\left[e_{AC}(t)\cdot\cos(\omega_1 t)\right] * g_{DC}(t)\right\}\cdot\cos(\omega_1 t) + \left\{\left[e_{AC}(t)\cdot\sin(\omega_1 t)\right] * g_{DC}(t)\right\}\cdot\sin(\omega_1 t) \quad (1)$$

From the above description, a transfer function in stationary frame $G_{AC}(s)$ which provides the same frequency responses as (1) can be determined. To figure out the function of $G_{AC}(s)$, some derivations need to be done. The system in this form can be presented by

$$V_{AC}(t) = G_{AC}(s)E_{AC}(s) \quad (2)$$

The time domain description of (2) is

$$v_{AC}(t) = e_{AC}(t) * g_{AC}(t) \quad (3)$$

Where ω_1 is the fundamental frequency. To simplify the following mathematics two functions are defined:

$$f_1(t) = g_{DC}(t) * \left(e_{AC}(t) \cdot \cos(\omega_1 t)\right) \tag{4}$$

$$f_2(t) = g_{DC}(t) * \left(e_{AC}(t) \cdot \sin(\omega_1 t)\right) \tag{5}$$

The Laplace transforms of f_1 and f_2 are

$$\begin{aligned} F_1(s) &= \ell\left\{g_{DC}(t) * \left[e_{AC}(t) \cdot \cos(\omega_1 t)\right]\right\} \\ &= G_{DC}(s) \cdot \ell\left\{e_{AC}(t) \cdot \cos(\omega_1 t)\right\} \\ &= \frac{1}{2} G_{DC}(s)\left\{E_{AC}(s + j\omega_1) + E_{AC}(s - j\omega_1)\right\} \end{aligned} \tag{6}$$

$$\begin{aligned} F_2(s) &= \ell\left\{g_{DC}(t) * \left[e_{AC}(t) \cdot \sin(\omega_1 t)\right]\right\} \\ &= G_{DC}(s) \cdot \ell\left\{e_{AC}(t) \cdot \sin(\omega_1 t)\right\} \\ &= \frac{1}{2} G_{DC}(s)\left\{E_{AC}(s + j\omega_1) - E_{AC}(s - j\omega_1)\right\} \end{aligned} \tag{6}$$

Then the mathematical description of the system can be broken into two components A and B, and by using the modulation theorem of the Laplace transform and the function f_1 and f_2, the Laplace transform of each component can be derived as follow:

$$\begin{aligned} A &= \ell\left\{\left[\left(e_{AC}(t) \cdot \cos(\omega_1 t)\right) * g_{DC}(t)\right]\cos(\omega_1 t)\right\} \\ &= \ell\left\{f_1(t) \cdot \cos(\omega_1 t)\right\} \\ &= \frac{1}{2}\left\{F_1(s + j\omega_1) + F_1(s - j\omega_1)\right\} \\ &= \frac{1}{4}\left\{\begin{array}{l} G_{DC}(s + j\omega_1)\left\{E_{AC}(s + 2j\omega_1) + E_{AC}(s)\right\} \\ + G_{DC}(s - j\omega_1)\left\{E_{AC}(s) + E_{AC}(s - 2j\omega_1)\right\} \end{array}\right\} \end{aligned} \tag{7}$$

$$\begin{aligned} B &= \ell\left\{\left[\left(e_{AC}(t) \cdot \sin(\omega_1 t)\right) * g_{DC}(t)\right]\sin(\omega_1 t)\right\} \\ &= \ell\left\{f_1(t) \cdot \sin(\omega_1 t)\right\} \\ &= \frac{j}{2}\left\{F_1(s + j\omega_1) - F_1(s - j\omega_1)\right\} \\ &= \frac{1}{4}\left\{\begin{array}{l} -G_{DC}(s + j\omega_1)\left\{E_{AC}(s + 2j\omega_1) - E_{AC}(s)\right\} \\ + G_{DC}(s - j\omega_1)\left\{E_{AC}(s) - E_{AC}(s - 2j\omega_1)\right\} \end{array}\right\} \end{aligned} \tag{8}$$

It can be seen, both A and B contain the DC and double-frequency error component terms $E_{AC}(s)$ and $E_{AC}(s+2j\omega_1)$. Then the transformation based on DC transfer function $G_{DC}(s)$ can be expressed by summing A and B:

$$\begin{aligned} V_{AC} &= A + B \\ &= \frac{1}{4}\left\{2\left\{G_{DC}(s + j\omega_1) + G_{DC}(s - j\omega_1)\right\} \cdot E_{AC}(s)\right\} \\ &= \frac{1}{2}\left\{G_{DC}(s + j\omega_1) + G_{DC}(s - j\omega_1)\right\} \cdot E_{AC}(s) \end{aligned} \tag{9}$$

According to equations (2) and (9), the stationary frame transfer function can be obtained.

$$G_{AC} = \frac{1}{2}\left\{G_{DC}(s + j\omega_1) + G_{DC}(s - j\omega_1)\right\} \tag{10}$$

It is worth noting that equation (10) is a general expression which allows the generation of the frequency response of the regulator (1) for any given DC regulator transfer function $G_{DC}(s)$, and when the reference signal bandwidth is smaller than the reference frequency itself, the equation (10) can be further simplified as equation (11) to provide a more convenient implementation.

$$G_{AC} = G_{DC}\left(\frac{s^2 + \omega_1^2}{2s}\right) \tag{11}$$

This paper mainly focuses on the relationship between PI controller and PR controller, so when using equation (11) and the transfer function $G_{DC}(s)=K\text{p}+K\text{i}/s$, the equivalent stationary frame PR controller transfer function can be obtained.

$$G_{AC} = G_{DC}\left(\frac{s^2 + \omega_1^2}{2s}\right) = K_p + \frac{2K_i s}{s^2 + \omega_1^2} = K_p + \frac{K_r s}{s^2 + \omega_1^2} \tag{12}$$

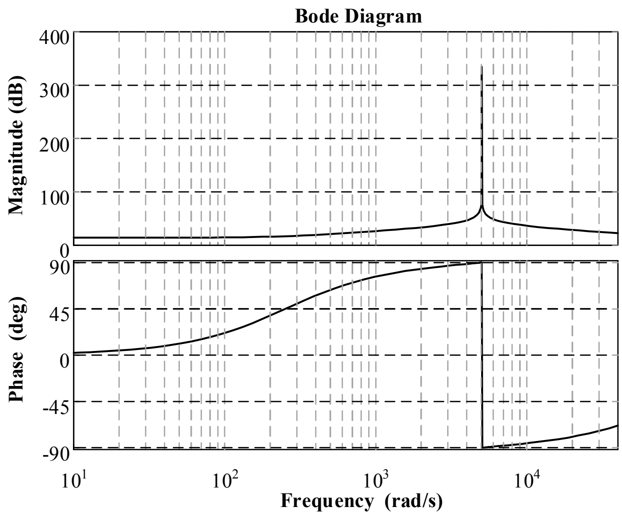

Fig. 3 Frequency responses of PR controller for variation in Kp=6 and ω1=2π*800

When K_p=5 and ω_1=2π*800, the Bode diagram is shown in Fig. 3. It can be seen from the figure that when the output signal is at the resonant frequency ω_1, its gain is infinite, making the steady-state error of the output of the inverter system to be zero static error tracking of the AC signal. According to the analysis and derivation, a frequency adaptive multi-harmonic PR controller is introduced and the structure of it is illustrated in Fig 4. The frequency ω_1 is the frequency of the aircraft power system which obtained by PLL, hence the PR control has the capability of frequency adaption. The ω_2, $\omega_3 \ldots \omega_n$ are the frequencies of injected harmonic currents. The multi-harmonic PR controller is used to achieve simultaneous multiple harmonic current injection. The current reference compared with the actual gird current and then the difference is sent into the PR controller which then output the reference value of gird voltage.

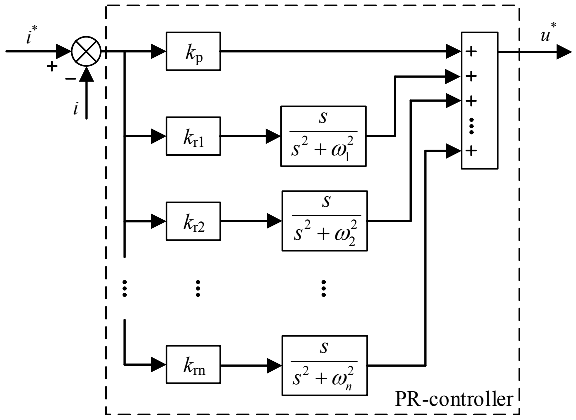

Fig 4. Frequency adaptive multi-harmonic proportional resonance controller

B. The scheme of proposed control strategy

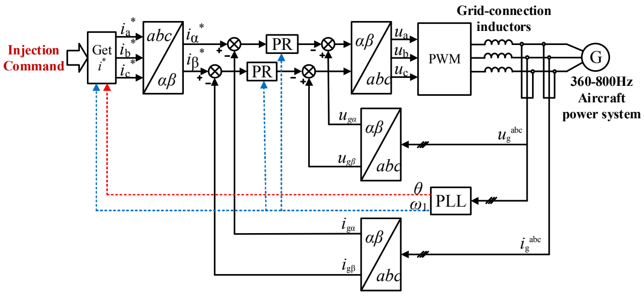

Fig 5. Overall control strategy based on PR controller

The overall block diagram of the algorithm is shown in Fig 5. According to the grid information and the injection command, the reference value of the three-phase harmonic current (i_a^*, i_b^*, i_c^*) can be calculated. The α-β transformation is applied to transfer i_a^*, i_b^*, $i_c^*$to i_α^*, i_β^* which then compared with the actual value i_α, i_β. The error is sent into the frequency adaptive multi-harmonic proportional resonance controller as the input. The output of PR controller compared with the additional voltage and then the reference value is sent to the PWM modulator.

III. Topology and System Overview of HCG

For the fundamental frequency of MEA electrical power system is at the range of 360-800Hz, injecting the harmonic component up to 40 times of fundamental frequency means the highest frequency is up to 32kHz and the equivalent switching frequency should be not lower than 800kHz. Due to the high frequency of the output, the switching frequency of the conventional IGBT, MOSFET can hardly meet the requirement. In this paper, the wide band-gap semiconductor device GaN HFET is applied. For the topology selection of HCG, there are two necessary factors need to be considered:

i. The high price of GaN devices; to control the cost of the whole system, the number of GaN devices should be as few as possible.

ii. The high frequency of control system; the selected topology should avoid the use of the structures with floating capacitor and bus segmented to reduce the controller's algorithm burden.

Considering all above conditions, the cascaded H-bridge topology is selected to achieve the high frequency harmonic injection. The system diagram of the proposed HCG is illustrated in figure 6. The HCG connected to the onboard power system through the grid-connected reactors. and receive the injection command to achieve harmonic current generation.

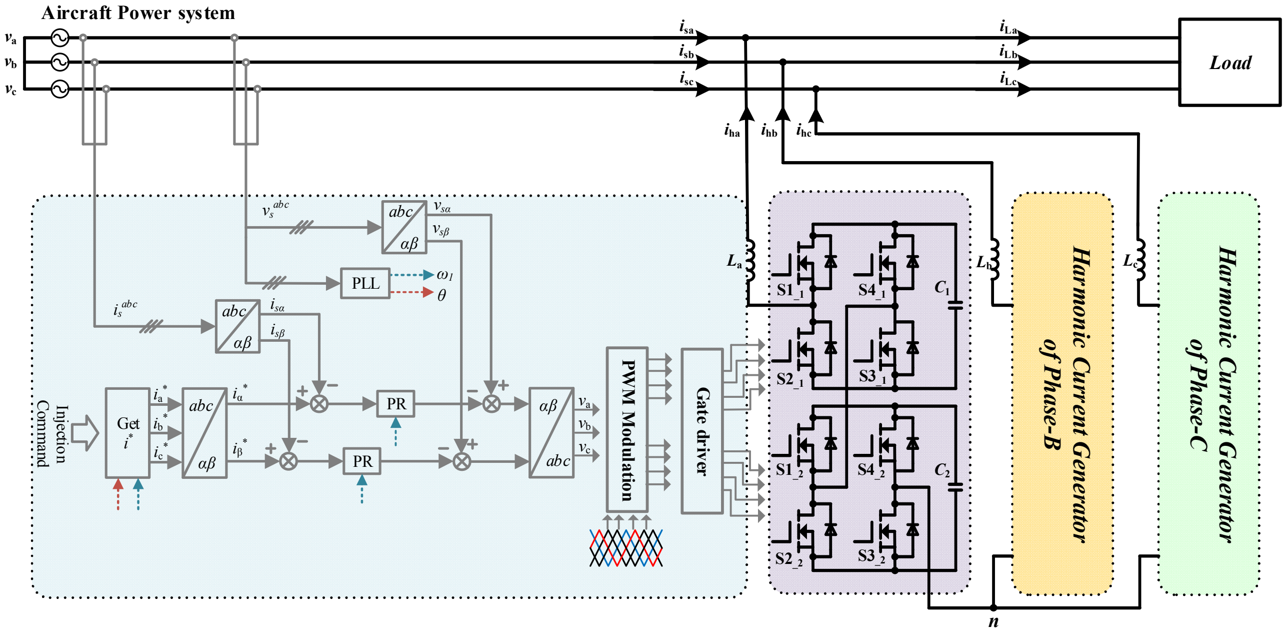

Fig 6. System diagram of the proposed harmonic current generator

IV. SIMULATION RESOULTS OF PROPOSED HCG AND PROTOTYPE

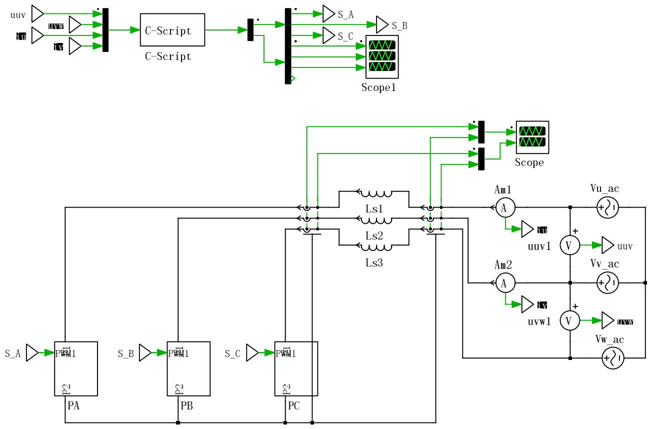

Fig 7. Simulation model of HCG

In order to verify the proposed algorithm under various operating conditions, a simulation model is built in the PLECS simulation environment (shown in figure 7). The control strategy is implemented in C-Script, which is convenient for algorithm migration. Table I illustrates the simulation parameters.

TABLE I. PARAMETERS OF SIMULATION

Parameter	**Value**
Gird-connection inductor	505μH
Switching frequency	400kHz
Frequency of aircraft EPS	360-800Hz
Line voltage (rms) of aircraft EPS	380V
harmonic current amplitude	11A

A. Harmonic Generator Standby Mode Simulation Results

Figure 7 shows the simulation waveforms of the harmonic generator in standby mode (the on-board power grid frequency is set to 400Hz). From the top to the bottom of the figure are: Phase-A output voltage of cascaded H-bridge topology, on-board power grid three-phase voltage, on-board power grid three-phase current, voltage drop across phase-A grid-connected reactor. It can be seen that under the standby condition, the current of the aircraft power gird is basically zero and there is only a small fluctuation in the switching frequency.

Figure 8 shows the results of 4th harmonic current injection (with the same onboard grid frequency of the standby mode). It can be seen that in the low-order harmonic injection mode, the HCG control strategy realizes the perfectly current tracking which can be proved in figure 8 (the figures show no flotation and the grid side current follows the command value perfectly). The simulation results of 40th harmonic current injection of the HCG is illustrated in figure 9, in which the frequency of the aircraft power system is set at 400 Hz. The results have the same order as figure 7 and 8. It can be seen, when injecting higher frequency harmonic, both the current and voltage maintain a stable state and no fluctuation appear. The control system shows a good performance.

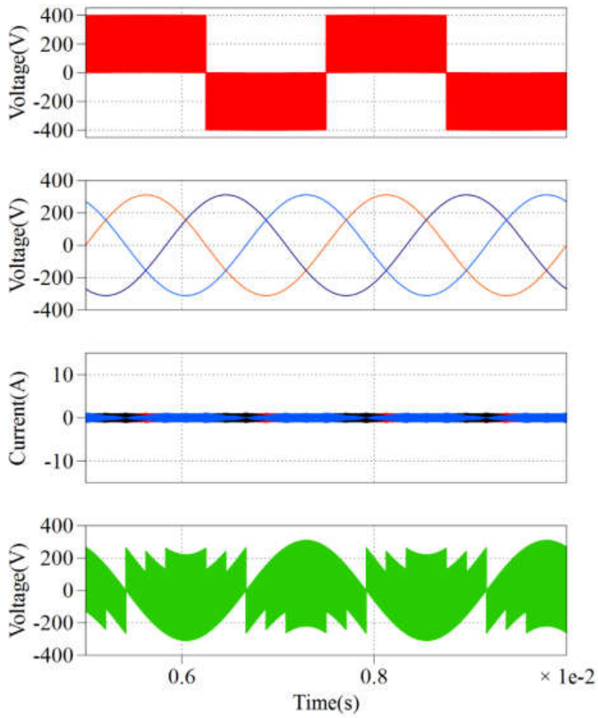

Fig 7. Standby Simulation Results of proposed HCG

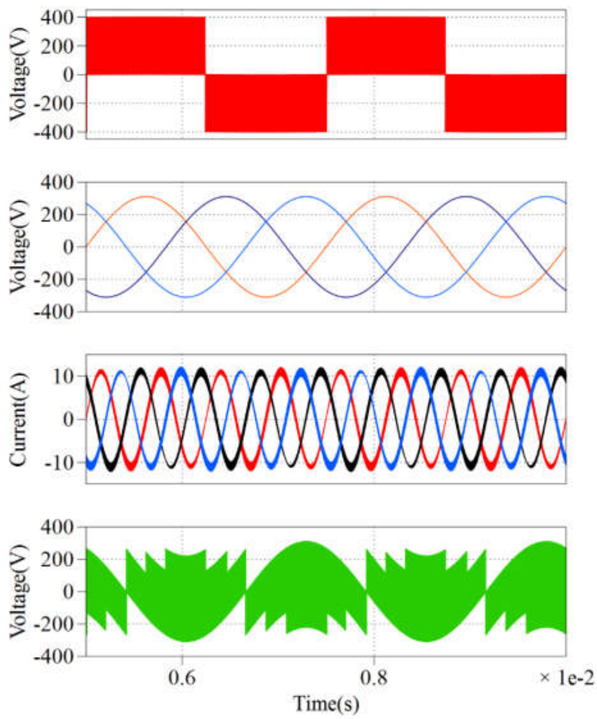

Fig 8. Low-order harmonic injection simulation results

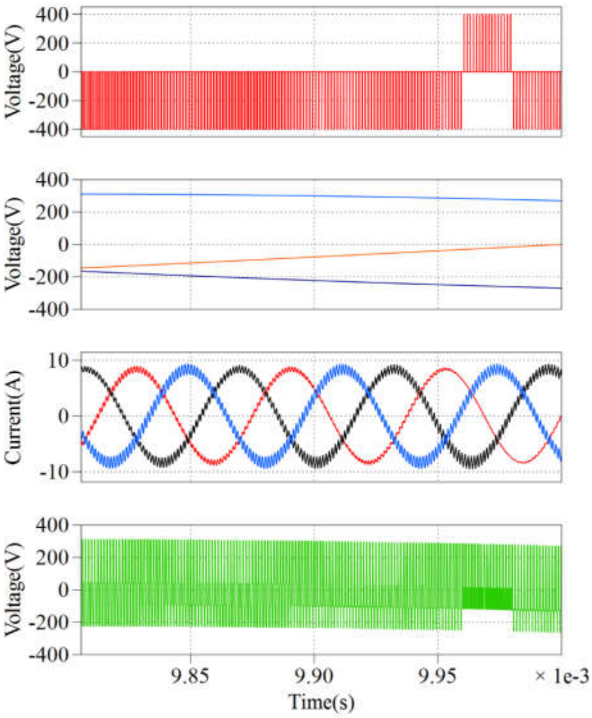

Fig 9. High-order harmonic injection simulation results

B. *Prototype of HCG in laboratory*

Based on the theoretical analysis and design proposal, a 10kW prototype of the proposed HCG is built in laboratory (shown in figure 10). Since the frequency need to up to 400 kHz, it is difficult for ordinary controllers to meet such high control performance requirements. Therefore, the Xilinx ZYNQ processor is used as the core controller for the platform. By tightly integrating the dual ARM Cortex-A9 MPCore with

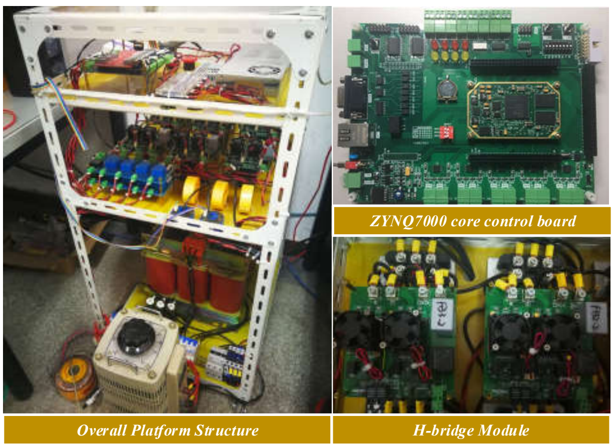

Fig 10. 10kW prototype of the proposed HCG

a programmable logic and hardware peripheral IP, the Xilinx Zynq-7000 extensible processing platform (EPP) can provide greater flexibility, higher configurability and better processing performance. The designed Zynq-7000 core control board is illustrated in figure 10.

V. CONCLUTION

The development of more electric aircraft and all electric aircraft leads to an increasing number of power electronics in aircraft EPS. This will bring more and more harmonics to the on-board power grid, which cause serious problems such as low power quality and extra fuel cost, etc. In this paper, a high frequency harmonic current generator(HCG) for aircraft EPS is designed to provide a convenient method for onboard power quality researches. A frequency adaptive multi-harmonic proportional resonant controller is introduced to realize high frequency harmonics injection. Due to the high frequency of command harmonics which up to 800kHz, the GaN HFETs based cascaded H-bridge topology is selected. In order to verify the proposed algorithm, a simulation model was built in the PLECS simulation environment. The results under various operating conditions show a good performance of the proposed control strategy. At the end, based on the Xilinx ZYNQ processor and GaN devices, a 10kW prototype of the designed HCG is built in the laboratory and there are some further researches to be done in the future.

ACKNOWLEDGMENT

This work was supported by the Ningbo Science & Technology Bureau under Grant 2017D10029.

REFERENCES

[1] K. Emadi and M. Ehsani, "Aircraft power systems: technology, state of the art, and future trends," IEEE Aerosp. Electron. Syst. Mag., vol. 15, no. 1, pp. 28–32, 2000.

[2] J. A. Rosero, J. A. Ortega, E. Aldabas, and L. Romeral, "Moving towards a more electric aircraft," IEEE Aerosp. Electron. Syst. Mag., vol. 22, no. 3, pp. 3–9, 2007.

[3] E. Lavopa, P. Zanchetta, M. Sumner, and F. Cupertino, "Real-Time Estimation of Fundamental Frequency and Harmonics for Active Shunt Power Filters in Aircraft Electrical Systems," IEEE Trans. Ind. Electron., vol. 56, no. 8, pp. 2875–2884, 2009.

[4] A. Eid, H. El-Kishky, M. Abdel-Salam, and M. T. El-Mohandes, "On Power Quality of Variable-Speed Constant-Frequency Aircraft Electric Power Systems," IEEE Trans. Power Deliv., vol. 25, no. 1, pp. 55–65, 2010.

[5] V. Khadkikar, "Enhancing Electric Power Quality Using UPQC: A Comprehensive Overview," IEEE Trans. Power Electron., vol. 27, no. 5, pp. 2284–2297, 2012.

[6] S. O. R. Moheimani, B. J. G. Vautier, and B. Bhikkaji, "Experimental implementation of extended multivariable PPF control on an active structure," IEEE Trans. Control Syst. Technol., vol. 14, no. 3, pp. 443–455, 2006.

[7] N. He, D. Xu, and L. Huang, "The Application of Particle Swarm Optimization to Passive and Hybrid Active Power Filter Design," IEEE Trans. Ind. Electron., vol. 56, no. 8, pp. 2841–2851, 2009.

[8] J. Liu, P. Zanchetta, M. Degano, and E. Lavopa, "Control Design and Implementation for High Performance Shunt Active Filters in Aircraft Power Grids," IEEE Trans. Ind. Electron., vol. 59, no. 9, pp. 3604–3613, 2012.

[9] A. Bhattacharya and C. Chakraborty, "A Shunt Active Power Filter With Enhanced Performance Using ANN-Based Predictive and Adaptive Controllers," IEEE Trans. Ind. Electron., vol. 58, no. 2, pp. 421–428, 2011.

[10] J. He, Y. W. Li, and M. S. Munir, “A Flexible Harmonic Control Approach Through Voltage-Controlled DG–Grid Interfacing Converters,” IEEE Trans. Ind. Electron., vol. 59, no. 1, pp. 444–455, 2012.

[11] A. G. Yepes, F. D. Freijedo, Ó. Lopez, and J. Doval-Gandoy, “Analysis and Design of Resonant Current Controllers for Voltage-Source Converters by Means of Nyquist Diagrams and Sensitivity Function,” IEEE Trans. Ind. Electron., vol. 58, no. 11, pp. 5231–5250, 2011.

[12] D. G. Holmes, T. A. Lipo, B. P. McGrath, and W. Y. Kong, “Optimized Design of Stationary Frame Three Phase AC Current Regulators,” IEEE Trans. Power Electron., vol. 24, no. 11, pp. 2417–2426, 2009.

[13] R. Teodorescu, F. Blaabjerg, M. Liserre, and P. C. Loh, “Proportional-resonant controllers and filters for grid-connected voltage-source converters,” IEE Proc. - Electr. Power Appl., vol. 153, no. 5, pp. 750–762, 2006.

[14] D. N. Zmood and D. G. Holmes, “Stationary frame current regulation of PWM inverters with zero steady-state error,” IEEE Trans. Power Electron., vol. 18, no. 3, pp. 814–822, 2003.

[15] D. N. Zmood and D. G. Holmes, “Stationary frame current regulation of PWM inverters with zero steady state error,” in 30th Annual IEEE Power Electronics Specialists Conference. Record. (Cat. No.99CH36321), 1999, vol. 2, pp. 1185–1190 vol.2.